Cellulose (2015) 22:3161–3176
DOI 10.1007/s10570-015-0728-6

ORIGINAL PAPER

Use of surfactants in cellulose nanowhisker/epoxy nanocomposites: effect on filler dispersion and system properties

Zahra Emami · Qingkai Meng · Gholamreza Pircheraghi · Ica Manas-Zloczower

Received: 12 May 2015 / Accepted: 4 August 2015 / Published online: 14 August 2015

Abstract Cellulose nanowhiskers (CNWs) prepared via TEMPO mediated oxidation are used as biodegradable filler in an epoxy matrix. Since CNWs are hydrophilic and epoxy is hydrophobic, amphiphilic block copolymer surfactants are employed to improve the interactions between the filler and the matrix. The surfactants used are Pluronics, a family of triblock copolymers containing two poly(ethylene oxide) blocks and one poly(propylene oxide) block. In this study, Pluronic L61 and L121 with molecular weight of 2000 and 4400 g/mol and hydrophilic to lipophilic balance of 3 and 1 respectively, are used and their effect on the dispersion of CNWs in epoxy is discussed. The hydrophilic tails of Pluronics interact with the hydroxyl and carboxylic groups on the CNW surface and then these surfactant-treated CNWs are directly incorporated into epoxy by high speed mixing. The dispersion state of the surfactant-treated CNWs in epoxy is assessed by rheological measurements and the mechanical properties of the resulting composites are characterized by tensile test and dynamic mechanical thermal analysis. The Pluronic L61 treated CNW/epoxy composites show the highest storage modulus at high temperatures (about 77 % increases) indicative of improved interfacial interactions between the CNWs and the epoxy matrix. Also, an increase of around 10 °C in the glass–rubbery transition temperature of the L61 treated CNW/epoxy composite leads to potential application at higher service temperatures.

Keywords Cellulose nanowhiskers · Epoxy resin · Nanocomposites · High-temperature properties · Block copolymer surfactant

Z. Emami · Q. Meng · I. Manas-Zloczower (✉)
Department of Macromolecular Science and Engineering, Case Western Reserve University, 2100 Adelbert Road, Cleveland, OH 44106, USA
e-mail: ixm@case.edu

Z. Emami
Department of Plastics, Iran Polymer and Petrochemical Institute, PO Box 14965-115, Tehran, Iran

G. Pircheraghi
Department of Materials Science and Engineering, Sharif University of Technology, PO Box 11365-9466, Tehran, Iran

Introduction

In the last years, the need for strong adhesives to be used in different applications such as aerospace (Silva and Campilho 2012), automotive industry (Grant et al. 2009) and offshore oil pipelines (Souza and Reis 2013) is continually increasing. In terms of structural applications, the mechanical properties of selected adhesives are strongly dependent on operating temperature. Most of amorphous polymers and adhesives show a significant decrease in mechanical properties at the glass transition temperature (T_g) and consequently, the T_g is usually the system limiting service temperature.

Epoxy is one of the most important polymers which has been widely used as a transparent adhesive and surface protective coating material (Li et al. 2006; Tang et al. 2009; Souza and Reis 2013). As an important adhesive material, epoxy has several advantages such as low shrink during cure, excellent moisture resistance, good electrical properties and increased mechanical and fatigue strength. However, epoxy resins are temperature sensitive and a significant drop in mechanical properties is observed at high temperatures (Souza and Reis 2013; Reis et al. 2015). Therefore, increasing the T_g of epoxy adhesives as well as improving the mechanical properties above the T_g are crucial.

Nanoscaled crystalline cellulosic short fibers called cellulose nanowhiskers (CNWs) are an interesting material for developing bio-based nanocomposites because of the abundance and renewability of cellulosic resources (Siqueira et al. 2010; Cao et al. 2012; Xu et al. 2013).

Cellulose nanowhiskers can be extracted from various sources such as wood (Beck-Candanedo et al. 2005; Abe et al. 2007), cotton (Qin et al. 2011; Satyamurthy et al. 2011; Fan and Li 2012), sisal (Morán et al. 2008) and tunicine (Elazzouzi-Hafraoui et al. 2008; Sacui et al. 2014) which consist of both crystalline and amorphous regions. To reach high mechanical properties, it is important to extract the crystalline parts from the cellulose sources by different methods such as mechanical treatment (Alemdar and Sain 2008), acid hydrolysis (Sadeghifar et al. 2011) and TEMPO-mediated oxidation (Saito and Isogai 2008; Lin et al. 2012). Moreover, the aspect ratio of cellulose nanowhiskers is dependent on their sources and preparation method, which lead to different mechanical properties (Eichhorn et al. 2010). CNWs with high aspect ratio have lower percolation threshold related to the formation of a continuous 3D network.

TEMPO-mediated oxidation is a catalytic reaction which converts primary hydroxyl groups in cellulose at the C6 position to aldehyde and then into carboxylic groups (Aspler et al. 2013). High yield, high reaction rate, environmental friendly and low cost materials are some advantages of this method (Isogai et al. 2011). According to the method, 2,2,6,6-tetramethylpiperidine-1-oxyl radical (TEMPO), sodium bromide and sodium hypochlorite are used to convert polysaccharide fibers to polyuronic acid fibers (Saito et al. 2006). Also, TEMPO molecules can penetrate into amorphous regions of the polyuronic acid fibers (Isogai et al. 2011). The microsized fibers after TEMPO mediated oxidation can be converted into nanosized whiskers by using mild mechanical disintegration treatment such as ultrasonication and mechanical shearing (Chen et al. 2011).

Many studies have explored the use of CNWs as reinforcement in polymeric materials (Grunert and Winter 2002; Petersson and Oksman 2006; Dong et al. 2012). Nanocomposite properties are strongly affected by the state of nanofiller dispersion and filler-matrix interfacial interaction. Therefore, how to improve the dispersion of hydrophilic cellulose fibers (with three hydroxylic groups per repeating unit) into hydrophobic polymeric matrices has been a subject of many studies (Favier et al. 1995; Kim et al. 2009; Yang et al. 2013). Surface modification including physical and chemical methods is a particular way to improve the compatibility of incompatible systems. Stretching (Wang et al. 1994), calendaring (Semsarzadeh et al. 1984) and corona discharge (Bledzki et al. 1996) are some examples of physical modification methods; polymer grafting and esterification are some examples of chemical surface modification methods in which diverse functional groups are grafted on the surface of CNWs. Except for two surface modification methods mentioned heretofore, using surfactant in incompatible systems is another popular and much simpler method, usually referred to as non-covalent surface chemical modification (Habibi et al. 2010). Ljungberg et al. (2005) used surfactant treated cellulose whiskers in a polypropylene matrix and obtained improved filler dispersion due to weakening the interactions between whiskers. Bondeson (Bondeson and Oksman 2007) used an anionic surfactant at different concentrations to disperse CNWs in polylactic acid. Increasing the amount of surfactant resulted in improved filler dispersion. The results of mechanical testing showed a maximum in tensile modulus for a 1:1 surfactant to filler ratio at 5 wt% CNW loading.

Triblock copolymers of poly(ethylene oxide) (PEO) and poly(propylene oxide) (PPO) are widely used to compatibilize various fillers into bio-based polymeric matrices due to their low toxicity and high biodegradability (Singh et al. 2013; Tercjak et al. 2015). For the surfactants, poly(ethylene oxide) is the hydrophilic tails and poly(propylene oxide) is the hydrophobic middle block (Li et al. 2011). A wide range of molecular weight and PEO/PPO ratio are

available leading to different properties such as aqueous solubility, association behavior viscosity, surface tension and cloud point (Alexandridis and Hatton 1995).

The main objectives of this research are to evaluate the use of triblock copolymers as non-covalent surfactants in the dispersion of CNWs synthesized via TEMPO-mediated oxidation reaction in epoxy. The relationship between the state of dispersion and composite properties enhancement, especially at higher temperatures, is evaluated and a rationale for the surfactant characteristics affecting dispersion is proposed. The results of this research may suggest the criteria for right surfactant selection in CNW/polymer nanocomposites.

Experimental

Materials

Epoxy used in this study was a modified diglycidyl ether of bisphenol-A (DGEBA, L135i, Hexion) with an amine hardener (RIMH 1366, Hexion) supplied by Momentive Specialty Chemicals. TEMPO (2,2,6,6-tetramethylpiperidine-1-oxyl radical), sodium bromide (NaBr), sodium hydroxide and sodium hypochlorite (NaClO) solutions (available chlorine 10–15 %) were purchased from Sigma-Aldrich (St. Louis, USA). All chemicals are laboratory grade and used as received. Microcrystalline cellulose (MCC) purchased from Sigma-Aldrich was used as cellulose source. The amphiphilic surfactants Pluronic L61 and L121 which are triblock copolymers of poly(ethylene oxide) (PEO) and poly(propylene oxide) (PPO) with different molecular weights were also obtained from Sigma-Aldrich. The main properties of the surfactants are presented in Table 1. Chemical structures of all materials used in this study are shown in Scheme 1.

Preparation of CNW and surfactant-treated CNWs

CNWs were prepared by TEMPO-mediated oxidation method (Saito et al. 2007). Briefly, MCC (2 g) was dispersed in 200 mL deionized water containing dissolved TEMPO (32 mg) and NaBr (200 mg) under mild magnetic stirring. The reaction was initiated by dropwise adding NaClO solution (4 mmol NaClO per gram of MCC). The pH of the reaction system was kept at 10 for 4 h by adding 0.5 M NaOH aqueous solution. Then, the oxidized MCC was thoroughly washed with deionized water by centrifugation for three times. The oxidized MCC aqueous suspension was sonicated continuously by an ultrasonic processor (Sonics Materials Vibra Cell VCX500) for 30 min at 40 % amplitude with a 13 mm diameter tip to break the micro-sized oxidized MCC from bundles of nanowhiskers into individual CNWs. Finally, the CNW suspensions were freeze-dried by a lyophilizer (VirTis BenchTop 4 K model) for 3 days and dry samples were stored in a desiccator at room temperature for further use. To prepare surfactant-treated CNWs, desired amount of surfactant was added to the oxidized MCC aqueous suspension (Scheme 2) at an oxidized MCC/surfactant weight ratio of 1:1. The surfactant to filler ratio was chosen based on several reports in literature (Bondeson and Oksman 2007; Kim et al. 2009). The aqueous suspension was sonicated for 30 min at the same conditions as described earlier and then freeze-dried and stored similar to the untreated CNWs.

Composite samples preparation

Desired amount of filler (CNWs or surfactant-treated CNWs) in epoxy was mixed by an overhead mechanical mixer (IKA mixer) for 2 h at room temperature at a 2 wt% CNW loading based on the amount of epoxy.

Table 1 Characteristic properties of the used surfactants

	Chemical structure	Mw (g/mol)	%Ethylene oxide	CMC[a] (%wt)	HLB[b]
Pluronic L61	$(PEO)_2(PPO)_{30}(PEO)_2$	2000	10 (Alexandridis and Hatton 1995)	0.02[c]	3[d]
Pluronic L121	$(PEO)_4(PPO)_{69}(PEO)_4$	4400	10 (Alexandridis and Hatton 1995)	0.0004[c]	1[d]

[a] The critical micelle concentration (CMC) is based on dispersion of copolymer in water

[b] Hydrophilic lipophilic balance

[c] The CMC values are reported by Evers et al. (2000) and Batrakova et al. (2003) for Pluronic L61 and L121, respectively

[d] The HLB values are reported by Oh et al. (2004)

Scheme 1 Chemical structure of materials used in the study

Epoxy

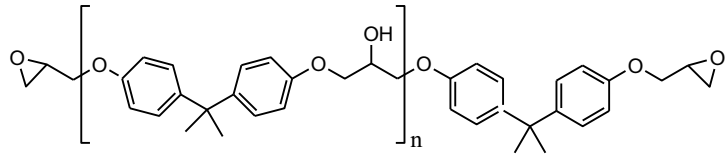

Cellulose nanowhiskers

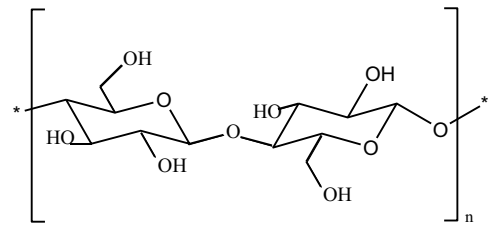

Pluronic L61

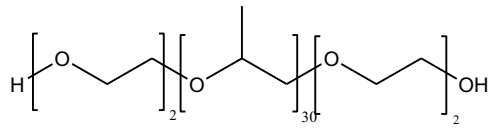

Pluronic L121

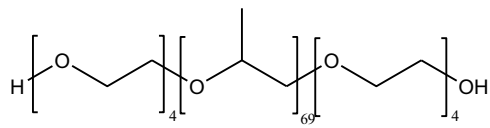

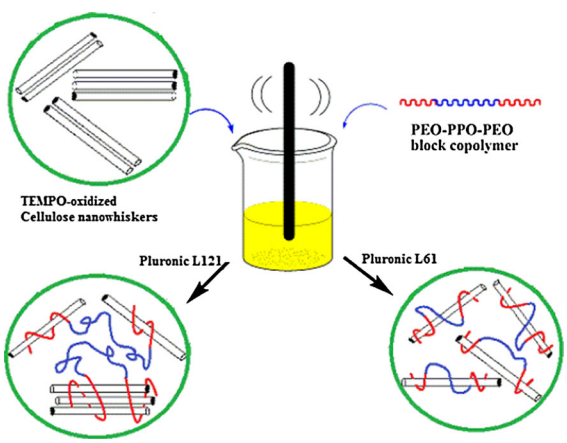

Scheme 2 Schematics for modification of TEMPO-oxidized cellulose nanowhiskers during sonication using different block copolymer surfactants

The mixtures were kept in a vacuum desiccator for 12 h for degassing and then they were sonicated in a pulse mode (5 s. on, 10 s. off) for 30 min at room temperature. Certain amount of hardener was added according to an epoxy/hardener weight ratio of 10:3 and the mixture was gently stirred for 5 min to uniformly mix the hardener with the epoxy while avoiding the trap of bubbles. After 5 min degassing in vacuum the mixture was poured into silicone molds for curing and shaping. The samples were cured at room temperature for 24 h and post-cured at 60 °C for 18 h. The cured samples were further polished according to the requirements on tensile testing sample dimensions.

Characterization

Atomic force microscopy (AFM)

CNWs were analyzed using an atomic force microscope (Veeco diMultiMode V, Veeco Instruments Inc, USA). One drop of diluted CNW aqueous suspension was dried on a silicon wafer. The equipment was operated in tapping mode using an antimony doped silicon probe (Bruker AFM probe, model TESP)

which has a resonant frequency and spring constant of 366–401 kHz and 20–80 N/m, respectively.

Thermal gravimetric analysis (TGA)

Thermogravimetric analysis of nanowhiskers and CNW/epoxy composites were carried out with a TGA instrument (TA Instruments Q500). About 7 mg of sample was put in a clean platinum pan and heated from room temperature to 600 °C at a rate of 10 °C/min under nitrogen atmosphere.

Tensile testing

Tensile properties of the composites were measured according to ASTM 638-03 standard using an Instron 1011 universal tensile tester at a crosshead speed of 1 mm/min at room temperature. The reported results are the average of seven measurements.

Rheology

Rheological properties of the CNW/epoxy suspension before curing were measured by a Thermo Scientific Haake Mars III rheometer at 27 °C. Experiments were carried out in both oscillatory and rotational shear modes with parallel plate geometry of 35 mm diameter and 1 mm measuring gap at 27 °C. A constant stress 0.1 Pa was used for oscillatory measurements, which was proved to be in the linear viscoelastic limit. Moreover, based on at least 3 repeating measurements the average error was found to be <15 %.

Dynamic mechanical thermal analyses (DMTA)

DMTA measurements were carried out with a TA Instruments DMA Q800 on rectangular samples with a size of 30 mm × ~4.7 mm × ~1.5 mm (length × width × thickness) in single cantilever mode with an oscillation frequency of 1 Hz and an oscillation amplitude of 15.0 μm. Measurements were carried out at a heating rate of 3 °C/min from room temperature up to 150 °C.

Scanning electron microscopy (SEM)

Tensile fracture surfaces of the composite samples were observed by a scanning electron microscope (JEOL JSM-6510LV) with an operating voltage of 30 kV. The fracture surfaces were sputter coated with gold.

Optical microscopy

The dispersion of different CNWs in epoxy matrix was observed using an Olympus BX51 optical microscope in different modes. Cross polarized images were used for better detection of the crystalline structure of cellulose nanowhiskers in epoxy.

Results and discussion

Synthesis and modification of CNWs

Figure 1 shows the AFM images of the CNWs prepared by TEMPO-mediated oxidation method. The dimensions of the nanowhiskers are determined based on 240 particles identified on multiple AFM height images (Fig. 1b). The average length and height of the prepared CNWs are 242.5 ± 48.3 and 4.2 ± 1.6 nm, respectively, corresponding to an average aspect ratio of 57.7. It is worth mentioning that TEMPO mediated oxidation causes defects in the amorphous phase of the MCC particles, which leads to the easy breakdown of the MCC particles into nanosized whiskers with mild mechanical treatment (Isogai et al. 2011). However, the dimensions and aspect ratio of our CNWs are similar to those values reported in literature for cellulose nanowhiskers extracted from wood (Kalia et al. 2011). Critical percolation volume fraction (Φc) of rod-like cellulose nanowhiskers can be calculated by $\phi_c = 0.7/\eta$ where $\eta = l/d$ is the aspect ratio of the filler and l and d are the average length and height of the filler, respectively (Tang and Weder 2010). Thus, in this case the critical percolation threshold of the CNWs is calculated to be 1.2 vol%. CNW concentration of all composite samples in this study (2 wt% equivalent to 1.5 vol% considering 1.14 g/cm^3 for epoxy density and 1.46 g/cm^3 for the density of crystalline cellulose nanowhiskers as reported by Sun (2005) and Capadona et al. (2009)) is above the calculated percolation threshold.

Figure 2 shows the TGA curves of the CNWs and surfactant-treated CNWs, while the inset graph displays the curves in the range from room temperature to 250 °C. The surfactant-treated CNWs have two clear

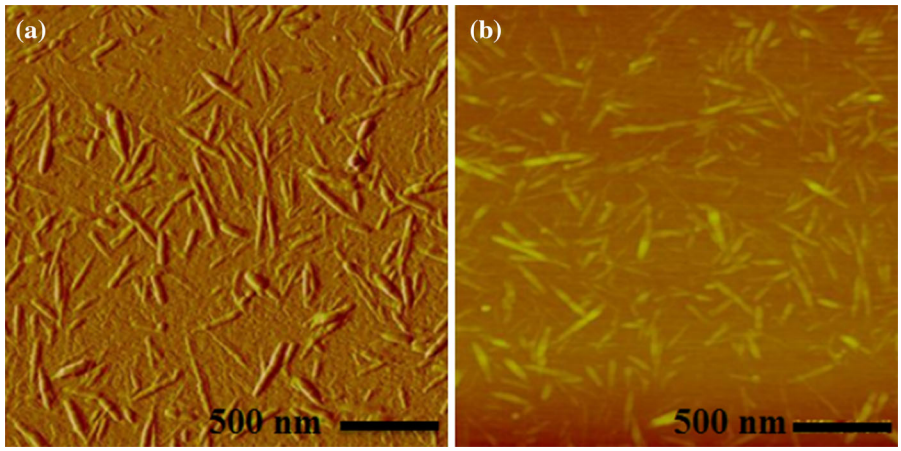

Fig. 1 AFM images of cellulose nanowhiskers prepared by TEMPO-mediated oxidation, **a** amplitude image and **b** height image

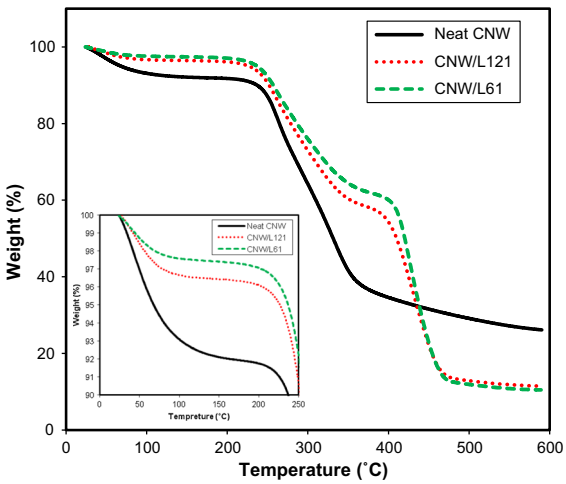

Fig. 2 Thermogravimetric curves for untreated and surfactant treated CNWs

weight loss steps: the first one is attributed to the decomposition of the cellulose and the other one is from the decomposition of the surfactants. By comparing the temperature in which sample degradation starts, it is obvious that L61 treated CNW has higher degradation temperature, indicative of better surfactant coverage of the filler preventing their fast degradation. The thermographs of the CNWs and surfactant-treated CNWs have been used to calculate the amount of surfactants (Pluronic L61 and L121) in the surfactant-treated CNWs (Table 2). In the inset graph, mass losses at the beginning of the TGA curves related to the evaporation of water are observed (Li et al. 2009). Due to the covering of CNW with

Table 2 Moisture and surfactant contents for CNWs and surfactant-treated CNWs

Filler	Moisture adsorbed (wt%)	Surfactant content (wt%)
Neat CNWs	8.04	0
Pluronic L121-treated CNWs	3.55	44.14
Pluronic L61-treated CNWs	2.54	48.87

surfactant the amount of adsorbed water in the modified CNWs significantly decreased, as shown in Table 2. Interaction of carboxylic and hydroxyl groups of the cellulose nanowhiskers with the hydrophilic part (ethylene oxide moieties) of the surfactant results in less moisture adsorption by hydrogen bonding of these functional groups with environmental water molecules. Moreover, the hydrophobic part of the surfactant/block copolymer can also cover the CNWs surface and suppresses the interaction with water molecules, preventing moisture adsorption. As shown in Table 2, the amount of the adsorbed moisture in the CNW sample treated with L61 block copolymer is lower than that of the sample treated with L121 block copolymer suggestive of better interaction of the L61 with CNWs.

Dispersion state of CNWs in epoxy suspensions

Figure 3 shows the optical micrographs and corresponding cross polarized images for dispersions of different CNWs in epoxy matrix before addition of the

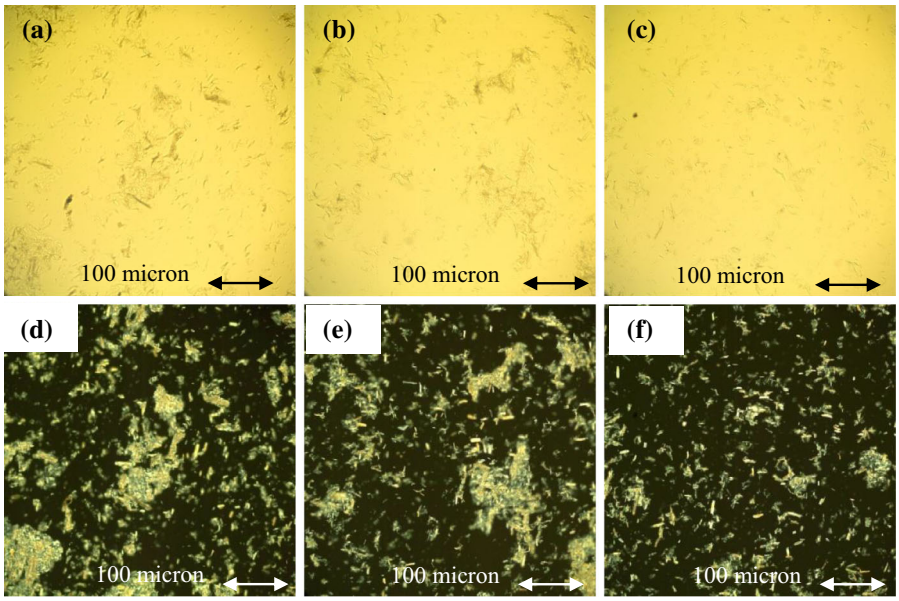

Fig. 3 Optical micrographs and corresponding cross polarized images of epoxy suspensions containing different CNWs, **a**, **d** non treated CNW, **b**, **e** L121 treated CNW and **c**, **f** L61 treated CNW (the optical and polarized micrographs were taken at the same magnification)

curing agent. Due to limited magnification of the optical instruments, optical micrographs cannot detect individual or small bundles of dispersed CNWs, but can be used to characterize the state of aggregation and network formation. Moreover, due to the crystalline structure of cellulose nanowhiskers, cross polarized images are more sensitive in distinguishing the state of dispersion.

While a network of large and dense CNWs aggregates is observed in the cross polarized image of the untreated CNW/epoxy suspension (Fig. 3d), a more uniform dispersion of small CNWs bundles can be detected in the L61 treated CNWs containing sample (Fig. 3f). The state of dispersion in the L121 treated CNWs suspension (Fig. 3e), is more similar to the untreated CNW/epoxy suspension showing the presence of the large aggregates and coarse dispersion. The optical and polarized micrographs of different samples demonstrate potential benefits of using the surfactant Pluronic L61 in improving CNW dispersion in epoxy.

The state of dispersion of different CNWs in epoxy was also investigated by rheological measurements in different modes. Rheological measurements in rotational and oscillatory shear modes can be used for assessment of filler dispersion state at nanoscale and network formation in polymeric suspensions, respectively (Pircheraghi et al. 2015). Figure 4 shows the dependence of complex viscosity (η^*), storage modulus (G') and *tan* δ on the oscillatory frequency (ω) for different samples. Neat epoxy behaves like a Newtonian fluid as the η^* is independent of oscillatory frequency. The addition of Pluronic surfactants slightly affects the η^* and clearly decreases the G'. Addition of untreated CNWs increases both complex viscosity and storage modulus whereas the surfactant treated CNWs suspensions show lower storage modulus and complex viscosity than the CNW/epoxy sample, with the Pluronic L61 treated CNWs exhibiting higher values than the Pluronic L121/CNW sample. Moreover the *tan* δ values for the L121 treated CNW/epoxy suspension is above 1, whereas this value for the L61 treated CNW/epoxy suspension is lower than 1 in a wide range of frequencies indicating the formation of a 3D network of CNW fillers in this sample. Based on the oscillatory rheological measurements, as well as optical and polarized micrographs shown in Fig. 3, it seems that in the suspension sample containing untreated CNWs there is a more developed 3D filler network. However, the quality and strength of this network should be mainly affected by the state of CNW dispersion. In order to better understand and evaluate the effect of dispersion state on filler network strength/quality, rotational shear rheology was performed on these samples.

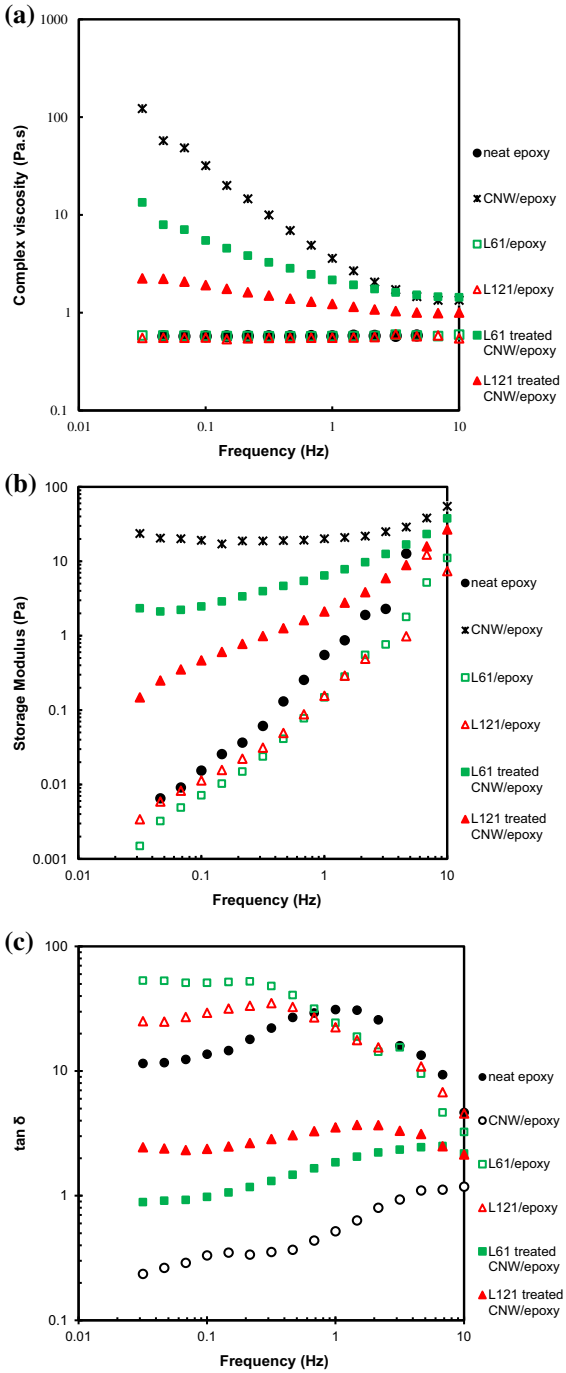

Fig. 4 Oscillatory measurement results for neat epoxy and cellulose nanowhisker/epoxy suspensions. **a** complex viscosity, **b** storage modulus and **c** tan δ versus frequency graphs

Literature reports indicate that rotational shear rheological measurements are more sensitive to nanoscale dispersion and the amount of individually dispersed nanofillers (Fan and Advani 2007; Pircheraghi et al. 2015) because a fragile network of filler can be easily destroyed by applied shear in these experiments (Fan and Advani 2007). Figure 5 shows shear viscosity dependence on shear rate for different suspension samples. Neat epoxy and samples containing surfactants without filler behave as Newtonian fluids. Addition of CNWs changed the shear characteristics of the samples. The L61 treated CNW/epoxy suspension sample shows the highest shear viscosity, whereas the untreated and L121 treated CNW suspensions display similar characteristics. These results point out to improved nanoscale dispersion in the L61 treated CNW suspension, whereas the L121 modified CNW/epoxy and the untreated CNW/epoxy suspensions are very similar. In other words, the amount of individually dispersed CNWs mostly responsible for the flow resistance in these samples is similar, indicating that Pluronic L121 could not act as an effective surfactant in this system.

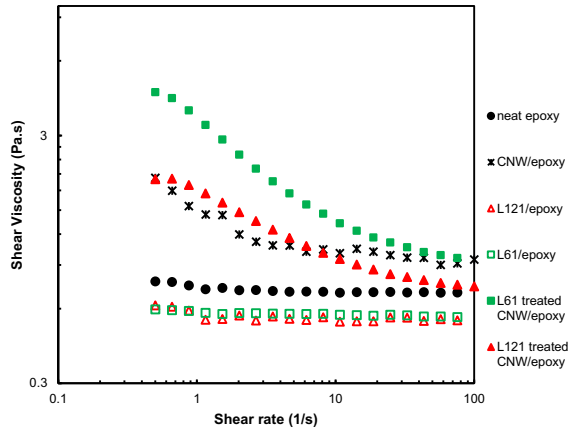

Fig. 5 Rotational shear data for neat epoxy and cellulose nanowhisker/epoxy suspensions

The rotational shear data can be fitted by a power law model, $\tau = k\dot{\gamma}^n$, with k the consistency index and n the power law index and the results are shown in Table 3.

The power-law index is around 1 for neat epoxy and samples containing Pluronic surfactants without filler, indicating Newtonian behavior. This behavior is changed to shear thinning in the suspension samples. However, the consistency and power law index are strongly dependent on filler loading and state of dispersion. While the CNW/epoxy sample showed the highest storage modulus in oscillatory rheology, its

Table 3 Flow parameters for neat epoxy and cellulose nanowhisker/epoxy suspensions

Samples	n	k	R^2
Neat epoxy	0.98	0.73	0.99
L121/epoxy	0.98	0.57	0.99
L61/epoxy	0.98	0.58	1
CNW/epoxy	0.89	1.45	0.99
L121 treated CNW/epoxy	0.79	1.70	0.99
L61 treated CNW/epoxy	0.68	3.20	0.98

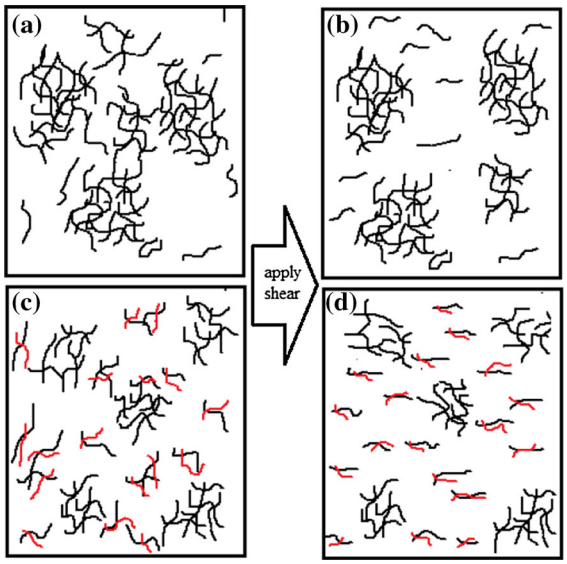

Fig. 6 Schematic behavior for CNW/epoxy sample **a** before shear and **b** after applying shear (order of 10 s^{-1}) and for the L61 treated CNW/epoxy sample **c** before shear and **d** after applying shear (order of 100 s^{-1})

consistency index is much lower than the L61 treated CNW/epoxy sample and is comparable with that of the L121 treated CNW/epoxy suspension. These results indicate less resistance against flow in these samples mainly due to poor nanoscale dispersion. On the other hand the lowest power law index in the L61 treated CNW suspension may correspond to more orientation ability of the well dispersed CNWs which results in enhanced shear thinning behavior (Bercea and Navard 2000; Eberle et al. 2008). These results reveal the role of the right surfactant selection in improving the CNW dispersion state and preventing re-aggregation (Ghorabi et al. 2012). Considering the optical microscopy and rheological measurement results, Fig. 6 illustrates a postulated schematic microstructure of the CNW/epoxy and L61 treated CNW/epoxy during oscillatory and shear measurements. The network consisting of large and fragile CNW aggregates in the CNW/epoxy sample, as revealed in the oscillatory rheology, can be easily destroyed under shear stress in rotational rheology, while the structure formed by small aggregates and well dispersed individual CNWs in the L61 treated CNW/epoxy suspension requires higher shear stress to destroy the network and orient the fillers.

Mechanical properties of CNW/epoxy composites below T_g

Mechanical properties of CNW epoxy composites are strongly affected by the formation of a 3D filler network above the percolation threshold (Tang and Weder 2010).

Figure 7 shows the tensile modulus, tensile strength and elongation at break of the neat epoxy and CNW/epoxy composites. Also shown are the tensile properties of the epoxy containing only surfactant. The tensile strength and elongation at break are lower for the surfactant containing epoxy samples, while the modulus remains similar with the neat epoxy. The addition of CNWs increases the tensile modulus in the untreated CNW/epoxy sample due to the rigidity of the rod-like CNWs but reduces the elongation at break and the tensile strength mainly because of uneven dispersion of the fillers and poor interfacial interactions between the highly hydrophilic CNW nanofillers and the epoxy matrix.

In the sample containing L121 treated CNWs the tensile modulus value is similar to the CNW/epoxy composite, while its tensile strength and elongation at break are slightly higher. The mechanical properties are highly improved in the L61 treated CNW/epoxy nanocomposites, mainly in terms of modulus and toughness, most likely due to improved dispersion and enhanced interfacial interaction between the block copolymer wrapped CNWs and the epoxy matrix. The hydrophilic tails of the surfactant hydrogen bond with the hydroxyl and carboxylic groups of the CNWs whereas the hydrophobic part can interact with the epoxy, which results in better interfacial interactions between the filler and the matrix. However, the magnitude of property enhancement is strongly affected by the state of CNW dispersion and strength of interaction between nanofiller and epoxy matrix via right selection of the block copolymer.

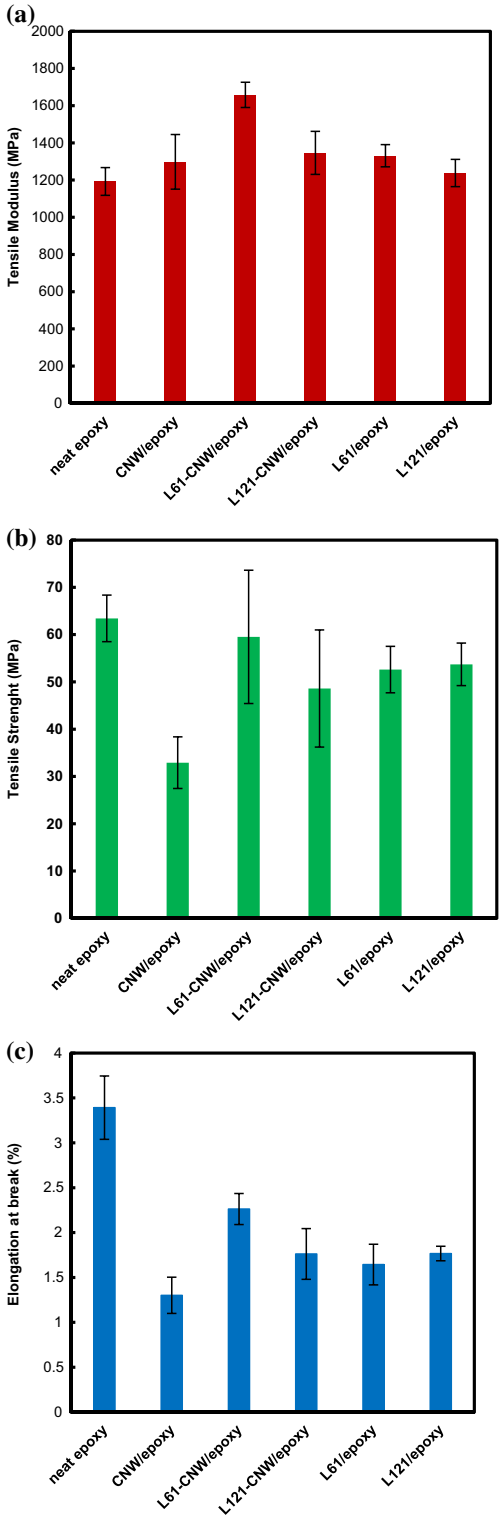

◀**Fig. 7** Tensile properties of the neat epoxy, epoxy with surfactant and different CNW/epoxy nanocomposites: **a** tensile modulus, **b** tensile strength and **c** elongation at break

It is noticeable that the trend in mechanical properties improvement in epoxy composites is in line with the shear rotational rheological properties, as shown in Fig. 5 and Table 3. This result points out to the role of individual or small bundles of CNWs dispersed at nanoscale in mechanical properties enhancement at room temperature, below the T_g of the epoxy matrix.

The tensile properties results may be also correlated with the CNW state of dispersion in the epoxy matrix. Due to strong intermolecular forces, mainly hydrogen bonding, CNWs usually form bundles of several whiskers or aggregates with an effective aspect ratio lower than the individually dispersed whiskers, especially when they are mixed in a hydrophobic matrix (Kim et al. 2009; Siqueira et al. 2010). The Young modulus results can be used to approximate filler effective aspect ratio in the composite by using an appropriate micromechanical model. The Halpin–Tsai model has been used successfully to calculate the modulus of different nanofiller reinforced polymer composites (Loos et al. 2012). For randomly oriented nanofiller in a polymer matrix, the modulus of the composite is given by the following equation:

$$\frac{E_c}{E_m} = \frac{3}{8}\left[\frac{1 + 2(l/d)\Psi_L V_f}{1 - \Psi_L V_f}\right] + \frac{5}{8}\left[\frac{1 + 2\Psi_T V_f}{1 - \Psi_T V_f}\right] \quad (1)$$

where

$$\Psi_L = \frac{(E_f/E_m) - 1}{(E_f/E_m) + 2(l/d)} \quad (2)$$

$$\Psi_T = \frac{(E_f/E_m) - 1}{(E_f/E_m) + 2} \quad (3)$$

Here, E_c, E_m, E_f are the elastic moduli of the composite, matrix and cellulose nanowhiskers, respectively, V_f is the CNW volume fraction and l/d is the effective aspect ratio of CNWs in the composite sample. Considering the measured values of the Young modulus for the different samples and taking

Table 4 Values of the elastic moduli of the composites and calculated effective aspect ratios

Sample code	E_m (GPa)	E_c (GPa)	Calculated effective aspect ratio (*l*/*d*)
CNW[a]/epoxy	1.19	1.3	6
L121 treated CNW/epoxy	1.19	1.34	10
L61 treated CNW/epoxy	1.19	1.66	70

[a] Aspect ratio (*l*/*d*) of CNWs as calculated from AFM is 57.7

the value of elastic modulus of individually dispersed cellulose nanowhiskers to be 143 GPa (Tang and Weder 2010; Loos and Manas-Zloczower 2013), the filler effective aspect ratio in different samples can be calculated and the results are reported in Table 4. The CNW volume fraction is 1.5 % for all samples.

The calculated effective aspect ratio for the L61 treated CNW/epoxy composite is in good agreement with the value obtained from AFM image analysis pointing out to the good dispersion of CNWs, mainly as individual whiskers in this sample. Thus, right surfactant selection resulted in nanoscale dispersion of CNWs and a nanocomposite with enhanced properties at low filler concentration.

Fracture surface morphology

Tensile fracture surface morphology of the composites was investigated by scanning electron microscopy (SEM) and the results are shown in Fig. 8. In the untreated CNW/epoxy composites, some aggregates in the range of 50 micron are observed, as indicated by the circles in Fig. 8a. These large aggregates with weak interfacial interaction/adhesion to the epoxy matrix can act as stress concentrating points and result in the formation and quick propagation of large cracks, as shown with arrows in Fig. 8b, and finally generate brittle fracture of the sample with decreased tensile strength under tensile load. Improved CNW dispersion can be achieved by using Pluronic L121 treated CNWs, but a CNW aggregate in the range of 10 micron is still observed as indicated by the circle in Fig. 8d. The fracture surface of this sample is rough and uneven (Fig. 8c), by comparison with the untreated CNW composite (Fig. 8a). However, in this sample the dispersion state is still not well improved and the interfacial interactions seem weak as evidenced by the formation of large cracks and voids under tensile load, as observed in Fig. 8d.

The composite containing Pluronic L61 treated CNWs shows the best CNW dispersion as indicated by less aggregates in the SEM images (Fig. 8e, f). Also, there is no evidence of voids and large cracks in this sample suggesting enhanced interfacial interaction/adhesion between L61 treated CNWs and epoxy matrix. Moreover, the fracture surface of this sample is very rough and uneven compared to the other samples and shows lots of microcrack formation and propagation, as indicated by the small arrows in Fig. 8e. This composite shows increased tensile toughness and the highest tensile strength among the composite samples.

These results reveal the important role of CNWs surface modification with the correctly selected surfactant in improving the CNWs dispersion state in polymeric matrices resulting in enhanced mechanical properties. Comparing the molecular characteristics of the two amphiphilic block copolymers used as surfactants in this work, it seems that the higher hydrophilic-lipophilic balance (HLB) of the L61 Pluronic surfactant can facilitate its interaction with the highly polar surface of the CNWs (as shown in Scheme 1), while its lower molecular weight prevents micelle formation at low concentration (Alexandridis and Hatton 1995) and may improve surfactant penetration inside the CNWs aggregates allowing surface modification and resulting in better dispersion in the epoxy matrix.

Mechanical properties of CNW/epoxy composites above T_g

Figure 9a shows flexural storage modulus (E') as a function of temperature for the neat epoxy and different composites. The glassy state of the composites is reflected by the plateau regime at low temperatures; by increasing temperature to T_g, the storage modulus decreases significantly followed by a rubbery

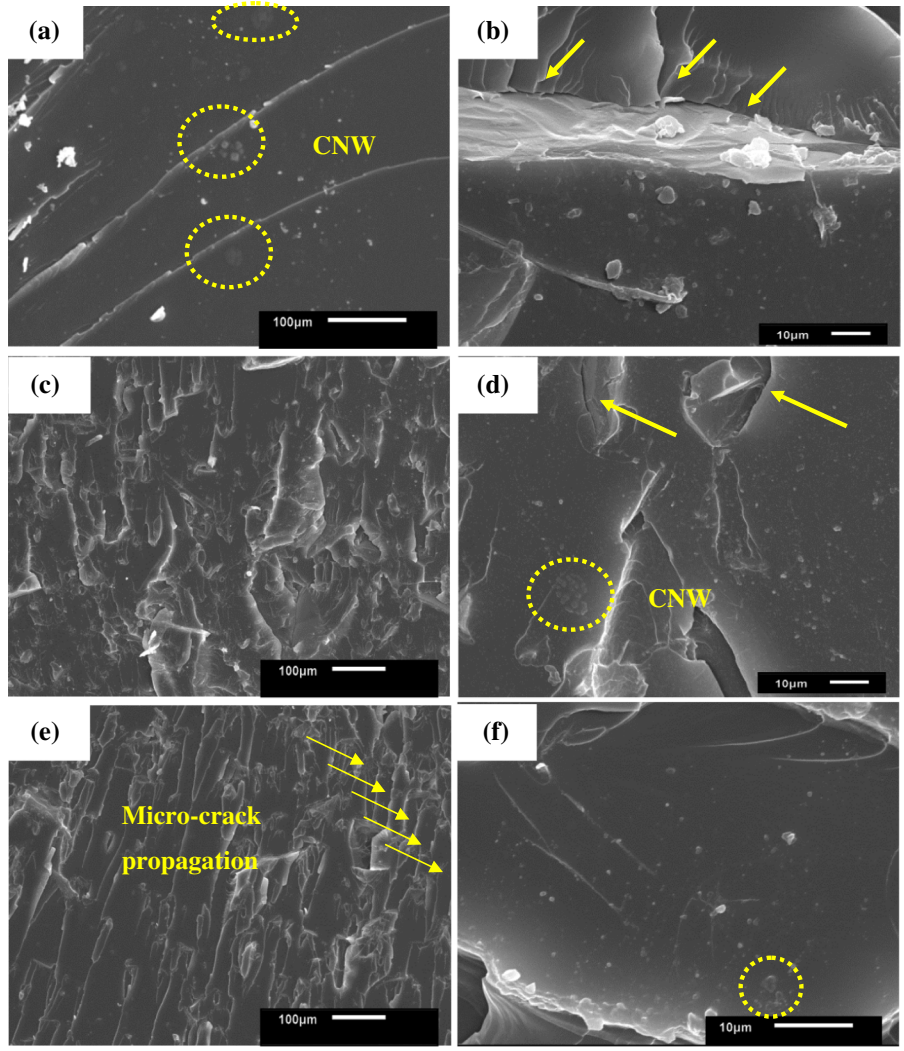

Fig. 8 SEM micrograph of **a**, **b** CNW/epoxy nanocomposite, **c**, **d** Pluronic L121 treated CNW/epoxy nanocomposite and **e**, **f** Pluronic L61 treated CNW/epoxy nanocomposite

plateau at high temperature. It should be mentioned that the response of the material in flexural mode is different than the tensile mode. Therefore, the storage modulus obtained from the DMTA measurements in flexural mode should not be compared with tensile modulus results reported earlier.

It is obvious that below the glass transition temperature the flexural storage modulus of the composite samples are almost identical, as shown in Table 5. Generally, because of the very similar elastic properties of the filler and epoxy polymer matrix in the glassy state, the presence of nanowhiskers does not affect the composite storage modulus to a great extent (Loos and Manas-Zloczower 2013). However, when adding untreated or Pluronic L61-treated CNWs to the neat epoxy the flexural storage modulus at 130 °C increases from 11.57 MPa for the neat epoxy to 15.5 and 20.63 MPa for the untreated and L61 treated CNW/epoxy composites, respectively, corresponding to about 34 and 78 % improvement. Several factors may contribute to the increased rubbery plateau modulus including: reinforcing effect by the CNWs, increased crosslink density and restricted mobility from enhanced polymer/whisker interactions. By contrast, the L121 treated CNW/epoxy composites shows a decrease in flexural storage modulus at

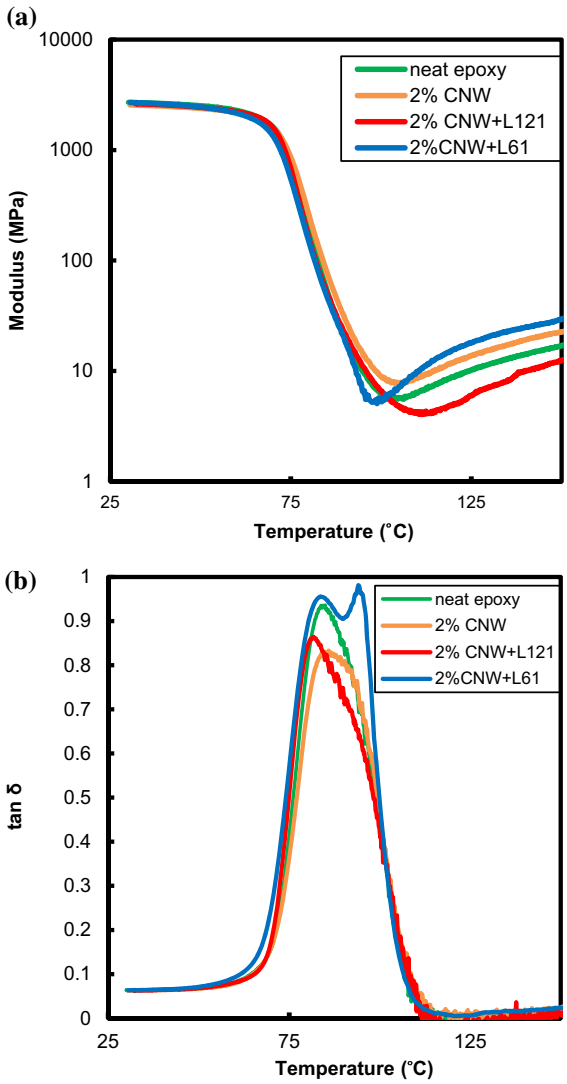

Fig. 9 **a** DMTA data of neat epoxy and cellulose nanowhisker/epoxy nanocomposites, **b** loss factor (tan δ) of neat epoxy and CNW/epoxy nanocomposites versus temperature

temperatures above the T_g of the epoxy matrix. Considering the higher affinity of the L121 surfactant towards the epoxy matrix due to its lower HLB and higher molecular weight by comparison with the L61 surfactant, it can be hypothesized that a significant portion of the L121 surfactant was not adsorbed by the CNWs but rather dispersed in the matrix. Also, considering the lower CMC of this surfactant (Table 1), micelle formation inside the epoxy matrix is possible (Ruiz-Pérez et al. 2008; Martin-Gallego et al. 2015). Such structures may act as toughening domains during tensile testing at room temperature in which the epoxy matrix is in its glassy state (Ruiz-Pérez et al. 2008). However, the dispersed surfactant chains or micelles inside the epoxy at temperatures above the T_g are very mobile and can acts as plasticizers facilitating the deformation and relaxation of the epoxy segments during dynamic flexural loading. This effect will compromise the reinforcing effect of rigid small CNW aggregates and consequently the storage modulus of the composite is reduced significantly. A comparison of the flexural storage moduli of all composites at low and high temperatures can be seen in Table 5.

Figure 9b shows tan δ as a function of temperature for the neat epoxy and the composites. A single peak is observed for both neat epoxy and the untreated CNW/epoxy composite and the temperature at the peak position is defined as the glass transition temperature (T_g). The incorporation of CNWs slightly increases the T_g, which can be related to weak filler/matrix interactions (Tang and Weder 2010) due to the low interfacial area of relatively large/micron sized aggregates as well as weak interfacial forces. The L121 treated CNWs in the composite shift the tan δ peak to a lower temperature, most likely due to possible surfactant micelle formation inside the matrix as well as low filler surface coverage, not facilitating effective matrix/filler interactions.

Mostly interesting the composite containing L61 treated CNWs shows two tan δ peaks: the first peak located at the same temperature as the neat epoxy (see Table 5), and the second peak at a temperature

Table 5 Glass transition temperature (T_g) and storage modulus (E') at low (35 °C) and high (130 °C) temperatures of neat epoxy and different CNW/epoxy nanocomposites based on DMTA results

Samples	E' (MPa) @ 35 °C	T_g (°C)	E' (MPa) @ 130 °C
Neat epoxy	2667	83.5	11.6
CNW/epoxy composite	2534.7	85.3	15.5
L121 treated CNW/epoxy composite	2603.2	80.5	7.2
L61 treated CNW/epoxy composite	2656.6	83.3–94.1	20.6

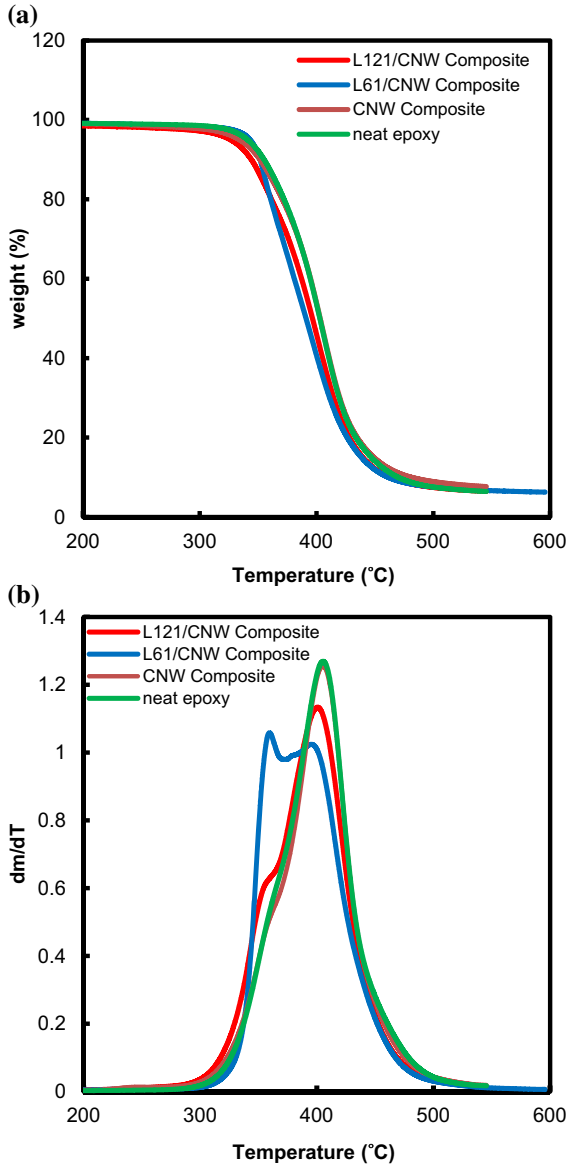

Fig. 10 **a** TGA data and **b** DTG curves for the neat epoxy and the CNW/epoxy nanocomposites containing treated and non-treated CNWs

10.6 °C higher than the T_g of the neat epoxy sample, which could be due to the restricted relaxation of some parts of the epoxy chains and network in the vicinity of the surfactant treated CNWs. These results confirm the higher efficiency of the Pluronic L61 surfactant in modifying the hydrophilic CNWs, shown in Scheme 2, and allowing for their better dispersion inside the lipophilic matrix with improved interfacial interactions. Similar behavior has been observed in a CNW/epoxy system modified with a nonylphenol ethoxylate nonionic surfactant (Cross et al. 2013).

Figure 10 shows the thermal degradation behavior of the neat epoxy and the composites. Since the decomposition of both the neat epoxy and the CNW/epoxy composites starts at 396 °C, the addition of 2 wt% of CNWs does not have any significant effect on the system thermal stability. In the derivative thermogravimetric (DTG) graph (Fig. 10b), the composites containing Pluronic L121 and L61 show a shoulder and a peak (around 360 °C) before the decomposition peak of the neat epoxy (400 °C), corresponding to the decomposition of CNWs. By contrast, the untreated CNW/epoxy composite does not show any shoulder or peak before the decomposition of the epoxy matrix. This result can be explained in terms of the presence of individual or small aggregates of CNWs in the surfactant treated CNW composites which can degrade easier than large agglomerates. The decomposition peak and shoulder are more pronounced in the L61 treated CNW composites, indicative of more individual and small aggregate units present in this sample. Thus TGA results also confirm the higher efficiency of the Pluronic L61 surfactant in dispersing CNWs in single or small aggregate units in epoxy.

Conclusions

Poor dispersion and low interfacial interactions between cellulose nanowhiskers (hydrophilic filler) and epoxy (hydrophobic matrix) have been observed in CNW/epoxy composites. PPO–PEO block copolymer surfactants (Pluronic L121 and Pluronic L61) are used in CNW/epoxy systems. Pluronic L61 treated CNW/epoxy composites show better mechanical and thermal properties than other composites, which can be attributed to the surfactant low molecular weight and high HLB allowing better filler coverage and enhanced filler/matrix interactions. The reinforcement effect of the Pluronic L61 treated CNWs in epoxy significantly increases at high temperatures, improving the potential applications of such composites in high temperature environment.

Acknowledgments We acknowledge the National Science Foundation for the financial support of our research through Grant PIRE-1243313.

References

Abe K, Iwamoto S, Yano H (2007) Obtaining cellulose nanofibers with a uniform width of 15 nm from wood. Biomacromolecules 8:3276–3278

Alemdar A, Sain M (2008) Isolation and characterization of nanofibers from agricultural residues: wheat straw and soy hulls. Bioresour Technol 99:1664–1671. doi:10.1016/j.biortech.2007.04.029

Alexandridis P, Hatton TA (1995) Poly(ethylene oxide)–poly(propylene oxide)–poly(ethylene oxide) block copolymer surfactants in aqueous solutions and at interfaces: thermodynamics, structure, dynamic, and modeling. Colloids Surf A Physicochem Eng Asp 96:1–46

Aspler J, Bouchard J, Hamad W et al (2013) Review of nanocellulosic products and their applications, 1st edn. Wiley, Hoboken

Batrakova EV, Li S, Alakhov VY et al (2003) Optimal structure requirements for pluronic block copolymers in modifying P-glycoprotein drug efflux transporter activity in bovine brain microvessel endothelial cells. J Pharmacol Exp Ther 304:845–854. doi:10.1124/jpet.102.043307

Beck-Candanedo S, Roman M, Gray DG (2005) Effect of reaction conditions on the properties and behavior of wood cellulose nanocrystal suspensions. Biomacromolecules 6:1048–1054. doi:10.1021/bm049300p

Bercea M, Navard P (2000) Shear dynamics of aqueous suspensions of cellulose whiskers. Macromolecules 33:6011–6016. doi:10.1021/ma000417p

Bledzki AK, Reihmane S, Gassan J (1996) Properties and modification methods for vegetable fibers for natural fiber composites. J Appl Polym Sci 59:1329–1336. doi:10.1002/(SICI)1097-4628(19960222)59:8<1329:AID-APP17>3.3.CO;2-5

Bondeson D, Oksman K (2007) Dispersion and characteristics of surfactant modified cellulose whiskers nanocomposites. Compos Interfaces 14:617–630. doi:10.1163/156855407782106519

Cao X, Ding B, Yu J, Al-Deyab SS (2012) Cellulose nanowhiskers extracted from TEMPO-oxidized jute fibers. Carbohydr Polym 90:1075–1080. doi:10.1016/j.carbpol.2012.06.046

Capadona JR, Shanmuganathan K, Trittschuh S et al (2009) Polymer nanocomposites with nanowhiskers isolated from microcrystalline cellulose. Biomacromolecules 10:712–716. doi:10.1021/bm8010903

Chen W, Yu H, Liu Y et al (2011) Individualization of cellulose nanofibers from wood using high-intensity ultrasonication combined with chemical pretreatments. Carbohydr Polym 83:1804–1811. doi:10.1016/j.carbpol.2010.10.040

Cross L, Schueneman G, Mintz E et al (2013) Nanocellulose reinforced epoxy elastomer. In: Proceeding of the annual meeting of the adhesion, pp 25–27

Dong H, Strawhecker KE, Snyder JF et al (2012) Cellulose nanocrystals as a reinforcing material for electrospun poly(methyl methacrylate) fibers: formation, properties and nanomechanical characterization. Carbohydr Polym 87:2488–2495. doi:10.1016/j.carbpol.2011.11.015

Eberle APR, Baird DG, Wapperom P (2008) Rheology of non-Newtonian fluids containing glass fibers: a review of experimental literature. Ind Eng Chem Res 47:3470–3488. doi:10.1021/ie070800j

Eichhorn SJ, Dufresne A, Aranguren M et al (2010) Review: current international research into cellulose nanofibres and nanocomposites. J Mater Sci 45:1–33. doi:10.1007/s10853-009-3874-0

Elazzouzi-Hafraoui S, Nishiyama Y, Putaux J-L et al (2008) The shape and size distribution of crystalline nanoparticles prepared by acid hydrolysis of native cellulose. Biomacromolecules 9:57–65. doi:10.1021/bm700769p

Evers R, Kool M, Smith AJ et al (2000) Inhibitory effect of the reversal agents V-104, and MRP2-mediated transport. Br J Cancer 83:366–374

Fan Z, Advani SG (2007) Rheology of multiwall carbon nanotube suspensions. J Rheol (N Y N Y) 51:585. doi:10.1122/1.2736424

Fan J, Li Y (2012) Maximizing the yield of nanocrystalline cellulose from cotton pulp fiber. Carbohydr Polym 88:1184–1188. doi:10.1016/j.carbpol.2012.01.081

Favier V, Chanzy H, Cavaille J (1995) Polymer nanocomposites reinforced by cellulose whiskers. Macromolecules 28:6365–6367

Ghorabi S, Rajabi L, Madaeni SS et al (2012) Effects of three surfactant types of anionic, cationic and non-ionic on tensile properties and fracture surface morphology of epoxy/MWCNT nanocomposites. Iran Polym J 21:121–130. doi:10.1007/s13726-011-0013-y

Grant LDR, Adam RD, da Silva LFM (2009) Effect of the temperature on the strength of adhesively-bonded single lab an T joints for the automotive industry. Int J Adhes Adhes 29:535–542

Grunert M, Winter WT (2002) Nanocomposites of cellulose acetate butyrate reinforced with cellulose nanocrystals. J Polym Environ 10:27–30

Habibi Y, Lucia LA, Rojas OJ (2010) Cellulose nanocrystals: chemistry, self-assembly, and applications. Chem Rev 110:3479–3500. doi:10.1021/cr900339w

Isogai A, Saito T, Fukuzumi H (2011) TEMPO-oxidized cellulose nanofibers. Nanoscale 3:71–85. doi:10.1039/c0nr00583e

Kalia S, Dufresne A, Cherian BM et al (2011) Cellulose-based bio- and nanocomposites: a review. Int J Polym Sci 2011:1–35. doi:10.1155/2011/837875

Kim J, Montero G, Habibi Y et al (2009) Dispersion of cellulose crystallites by nonionic surfactants in a hydrophobic polymer matrix. Polym Eng Sci. doi:10.1002/pen

Li Y-Q, Fu S-Y, Mai Y-W (2006) Preparation and characterization of transparent ZnO/epoxy nanocomposites with high-UV shielding efficiency. Polymer (Guildf) 47:2127–2132. doi:10.1016/j.polymer.2006.01.071

Li R, Fei J, Cai Y et al (2009) Cellulose whiskers extracted from mulberry: a novel biomass production. Carbohydr Polym 76:94–99. doi:10.1016/j.carbpol.2008.09.034

Li Y, Liu H, Song J et al (2011) Adsorption and association of a symmetric PEO–PPO–PEO triblock copolymer on polypropylene, polyethylene, and cellulose surfaces. ACS Appl Mater Interfaces 3:2349–2357

Lin N, Bruzzese C, Dufresne A (2012) TEMPO-oxidized nanocellulose participating as crosslinking aid for alginate-based sponges. ACS Appl Mater Interfaces 4:4948–4959. doi:10.1021/am301325r

Ljungberg N, Bonini C, Bortolussi F et al (2005) New nanocomposite materials reinforced with cellulose whiskers in atactic polypropylene: effect of surface and dispersion characteristics. Biomacromolecules 6:2732–2739. doi:10.1021/bm050222v

Loos MR, Manas-Zloczower I (2013) Micromechanical models for carbon nanotube and cellulose nanowhisker reinforced composites. Polym Eng Sci. doi:10.1002/pen

Loos MR, Yang J, Feke DL, Manas-Zloczower I (2012) Effect of block-copolymer dispersants on properties of carbon nanotube/epoxy systems. Compos Sci Technol 72:482–488. doi:10.1016/j.compscitech.2011.11.034

Martin-Gallego M, Verdejo R, Gestos A et al (2015) Morphology and mechanical properties of nanostructured thermoset/block copolymer blends with carbon nanoparticles. Compos Part A 71:136–143

Morán JI, Alvarez VA, Cyras VP, Vázquez A (2008) Extraction of cellulose and preparation of nanocellulose from sisal fibers. Cellulose 15:149–159. doi:10.1007/s10570-007-9145-9

Oh KT, Bronich TK, Kabanov AV (2004) Micellar formulations for drug delivery based on mixtures of hydrophobic and hydrophilic Pluronic® block copolymers. J Control Release 94:411–422. doi:10.1016/j.jconrel.2003.10.018

Petersson L, Oksman K (2006) Biopolymer based nanocomposites: comparing layered silicates and microcrystalline cellulose as nanoreinforcement. Compos Sci Technol 66:2187–2196. doi:10.1016/j.compscitech.2005.12.010

Pircheraghi G, Foudazi R, Manas-Zloczower I (2015) Characterization of carbon nanotube dispersion and filler network formation in melted polyol for nanocomposite materials. Power Technol 276:222–231

Qin Z-Y, Tong G-L, Chin YCF, Zhou J-C (2011) Preparation of ultrasonic-assisted high carboxylate content cellulose nanocrystals by tempo oxidation. BioResource 6:1136–1146

Reis JML, Amorim FC, da Silva AHMFT, da Costa Mattos HS (2015) Influence of temperature on the behavior of DGEBA (bisphenol A diglycidyl ether) epoxy adhesive. Int J Adhes Adhes 58:88–92. doi:10.1016/j.ijadhadh.2015.01.013

Ruiz-Pérez L, Royston GJ, Fairclough JPA, Ryan AJ (2008) Toughening by nanostructure. Polymer (Guildf) 49:4475–4488. doi:10.1016/j.polymer.2008.07.048

Sacui IA, Nieuwendaal RC, Burnett DJ et al (2014) Comparison of the properties of cellulose nanocrystals and cellulose nanofibrils isolated from bacteria, tunicate, and wood processed using acid, enzymatic, mechanical, and oxidative methods. ACS Appl Mater Interfaces 6:6127–6138. doi:10.1021/am500359f

Sadeghifar H, Filpponen I, Clarke SP et al (2011) Production of cellulose nanocrystals using hydrobromic acid and click reactions on their surface. J Mater Sci 46:7344–7355. doi:10.1007/s10853-011-5696-0

Saito T, Isogai A (2008) TEMPO-mediated oxidation of native cellulose. The effect of oxidation conditions on chemical and crystal structures of the water-insoluble fractions. Biomacromolecules 5:1983–1989

Saito T, Okita Y, Nge TT et al (2006) TEMPO-mediated oxidation of native cellulose: microscopic analysis of fibrous fractions in the oxidized products. Carbohydr Polym 65:435–440. doi:10.1016/j.carbpol.2006.01.034

Saito T, Kimura S, Nishiyama Y, Isogai A (2007) Cellulose nanofibers prepared by TEMPO-mediated oxidation of native cellulose. Biomacromolecules 8:2485–2491. doi:10.1021/bm0703970

Satyamurthy P, Jain P, Balasubramanya RH, Vigneshwaran N (2011) Preparation and characterization of cellulose nanowhiskers from cotton fibres by controlled microbial hydrolysis. Carbohydr Polym 83:122–129. doi:10.1016/j.carbpol.2010.07.029

Semsarzadeh M, Lotfali A, Mirzadeh H (1984) Jute reinforced polyester structures. Polym Compos 5:141–142

Silva MDBLEM, Campilho RDSG (2012) Effect of temperature on tensile strength and mode I fracture toughness of a high temperature epoxy adhesive. J Adhes Sci Technol 26:939–953

Singh V, Khullar P, Dave PN, Kaur N (2013) Micelles, mixed micelles, and applications of polyoxypropylene (PPO)-polyoxyethylene (PEO)-polyoxypropylene (PPO) triblock polymers. Int J Ind Chem 4:12. doi:10.1186/2228-5547-4-12

Siqueira G, Bras J, Dufresne A (2010) Cellulosic bionanocomposites: a review of preparation, properties and applications. Polymers (Basel) 2:728–765. doi:10.3390/polym2040728

Souza JPB, Reis JML (2013) Thermal behavior of DGEBA (Diglycidyl Ether of Bisphenol A) adhesives and its influence on the strength of joints. Appl Adhes Sci 1:1–10

Sun C (2005) True density of microcrystalline cellulose. J Pharm Sci 94:2132–2134. doi:10.1002/jps.20459

Tang L, Weder C (2010) Cellulose whisker/epoxy resin nanocomposites. ACS Appl Mater Interfaces 2:1073–1080. doi:10.1021/am900830h

Tang L, Whalen J, Schutte G, Weder C (2009) Stimuli-responsive epoxy coatings. ACS Appl Mater Interfaces 1:688–696. doi:10.1021/am800199u

Tercjak A, Gutierrez J, Barud HS et al (2015) Nano- and macroscale structural and mechanical properties of in situ synthesized bacterial cellulose/PEO-b-PPO-b-PEO biocomposites. ACS Appl Mater Interfaces 7:4142–4150. doi:10.1021/am508273x

Wang P, Liu J, Li R (1994) Physical modification of polyacrylonitrile precursor fiber: its effect on mechanical properties. J Appl Polym Sci 52:1667–1674

Xu X, Liu F, Jiang L et al (2013) Cellulose nanocrystals vs. cellulose nano fibrils: a comparative study on their microstructures and effects as polymer reinforcing agents. ACS Appl Mater Interfaces 5:2999–3009

Yang J, Zhao J, Xu F, Sun R (2013) Revealing strong nanocomposite hydrogels reinforced by cellulose nanocrystals: insight into morphologies and interactions. ACS Appl Mater Interfaces 5:12960–12967